Iraqi National Journal of Earth Science

www.earth.mosuljournals.com

Assessment of Limestone of Fatha Formation for Ordinary Portland cement industry in Zurbatiya Area, Eastern Iraq

Ahmad O. Al-Hadithi [1], Sattar J. Al-Khafaji [2*]

[1,2]*Department of Geology, College of Science, University of Basrah, Basrah, Iraq*

Article information

Received: 20- Apr -2024

Revised: 15- May -2024

Accepted: 20- June -2024

Available online: 01- Jul – 2025

Keywords:
Fatha Formation
Zurbatiyah
SEM
Clinker
OPC

Correspondence:
Name: Sattar J. Al-Khafaji
Email: Khafaji52000@gmail.com

ABSTRACT

Limestone deposits from the Fatha formation were assessed for the preparation of ordinary Portland cement. X-ray diffraction (XRD) analyses revealed that calcite is the most abundant mineral in limestone, followed by quartz, and a trace amount of dolomite. Chemical analyses by X-ray fluorescence (XRF) showed that the major oxides (CaO, SiO_2, Al_2O_3, Fe_2O_3, MgO, Na_2O, K_2O, TiO_2, SO_3, and P_2O_5) are within the acceptable limits required for the cement industry. Based on the chemical parameters of cement (LSF, SR, and AR), the mixture was made from limestone of the Fatha Formation and the claystone from the Injana Formation. Based on the chemical parameters of cement (LSF, SR, and AR), another mixture was prepared using limestone and claystone as in the first mixture, with the addition of sand and bauxite as corrective materials, to enhance the quality of the product. The mixture was burned at 1450°C by using a special program, and the produced clinker was assessed mineralogically and chemically to detect the major and minor phases of clinker. Bogue's equations indicated the percentage of (Alite, Billet, Aluminate, and Ferrite) within internationally accepted limits. Moreover, the Scanning electron microscopy (SEM) test indicates clear crystalline shapes of the clinker phases. The produced clinker has good quality and meets the required standard of ordinary Portland cement.

DOI: 10.33899/earth.2024.148980.1274,

تقييم الحجر الجيري لتكوين الفتحة لصناعة الاسمنت البورتلاندي الاعتيادي في منطقة زرباطية، شرق العراق

احمد اسامة الحديثي[1] ، **ستار جبار الخفاجي**[2*]

[2,1]قسم علوم الارض، كلية العلوم، جامعة البصرة، البصرة، العراق.

معلومات الارشفة

تاريخ الاستلام: 20- ابريل -2024

تاريخ المراجعة: 15- مايو -2024

تاريخ القبول: 20- يونيو -2024

تاريخ النشر الالكتروني: 01- يوليو -2025

الكلمات المفتاحية:
تكوين الفتحة
زرباطية
المجهر الماسح الالكتروني
كلنكر
اسمنت بورتلاندي اعتيادي

المراسلة:

الاسم: ستار جبار الخفاجي
Email: Khafaji52000@gmail.com

الملخص

تم تقييم رواسب الحجر الجيري من تكوين الفتحة، لتحضير الأسمنت البورتلاندي الاعتيادي. أظهرت تحاليل حيود الأشعة السينية (XRD) أن الكالسايت هو المعدن الأكثر وفرة في الحجر الجيري، يليه الكوارتز، وكمية ضئيلة من الدولومايت. أظهرت التحاليل الكيميائية بتحليل الأشعة السينية الوميضية (XRF) أن الأكاسيد الرئيسية (CaO، SiO_2، Al_2O_3، Fe_2O_3، MgO، Na_2O، K_2O، TiO_2، SO_3، وP_2O_5) تقع ضمن الحدود المقبولة المطلوبة لصناعة الأسمنت. بناءً على المعايير الكيميائية للأسمنت (LSF، SR، وAR)، تم تحظير خلطة من الحجر الجيري من تكوين الفتحة وأطيان من تكوين إنجانة. تم تحظير خلطة اخرى باستخدام الحجر الجيري والاطيان كما في الخلطة الأولى مع إضافة (الرمل والبوكسايت) كمواد تصحيحية وذلك لتحسين جودة المنتج. تم حرق الخليط عند درجة حرارة 1450 °م باستخدام برنامج حرق خاص، وتم تقييم الكلنكر المنتج معدنياً وكيميائياً للكشف عن الأطوار الرئيسية والثانوية للكلنكر. أشارت معادلات Bogue إلى نسب كل من (الأليت والبليت والألومينايت والفرايت) ضمن الحدود المقبولة عالميا. علاوة على ذلك، يشير اختبار المجهر الماسح الالكتروني (SEM) إلى الاشكال البلورية الواضحة لأطوار الكلنكر. يتمتع الكلنكر المنتج بجودة جيدة ويلبي المعايير المطلوبة للأسمنت البورتلاندي الاعتيادي.

DOI: 10.33899/earth.2024.148980.1274,

Introduction

The cement industry is a crucial industrial sector that plays a critical role in economic development (John, 2020). Cement is indispensable in building, engineering, construction, and civil engineering in general (Schorcht et al., 2013; Gambhir, 2013). Limestone, shale, chalk, or marl mixed with shale, clay, slate, blast furnace slag, silica sand, and iron ore are some of the primary raw materials that are utilized in the production of cement (Sengupta, 2020). Altering the composition of the mixture is accomplished by the utilization of a correction substance that is comprised of one of the key components of the mixture (Imam and Amin, 2007). To set up a cement factory, it is necessary to have a sufficient number of raw materials to meet the requirements and ensure the economic viability of the project. To investigate the industrial minerals found in the area under study, geologists conducted a great deal of research, geological surveys and field work, for examples of this are, the study by (Al-Fraji and Al-Khafaji 2023) focuses on evaluating the suitability of raw materials for the production of bricks and OPC from clay of Fatha Formation. Meanwhile, Al-Najjari and Al-Khafaji (2019) studied the petrography of sandstone in the Zurbatiyah area for the Injana Formation. (AL-Hadadi and AL-Khafaji, 2020) also studied the gypsum rocks of the Fatha formation in the study area. (Al-Ali and Al-Khafaji, 2020) studied the limestone rocks of the Ibrahim Formation and evaluated them as raw materials for the manufacture of ordinary Portland cement. (Khalaf and Al-Khafaji 2021) used

clay deposits in the area to manufacture low-cost and environmentally friendly bricks. (AL-Khafaji and AL-Hadadi, 2024) studied the industrial evaluation of mineral deposits in the Zurbatiyah area. The cement industry uses three chemical parameters for raw materials: LSF, SR, and AR. These parameters are very important in knowing whether the raw materials are suitable or not. This study aims to assess mineralogical and chemical properties of limestone deposits of Fatha formation for the manufacture of ordinary Portland cement and compare it with the international standard specification.

Geology and location of the study area

The study area is located in the district of Zurbatiyah in eastern Iraq within the Wasit governorate, which is 80 km west of the governorate center (Al Kut) between the latitudes 33º 08 ′ 60 ′ - 33º 23 ′ 57 ′ N and the longitudes 46º 02 60 ′ - 45º 58 15 ′ E. The study area represents the extreme margin of the low folded zone located between the High Mountain and Mesopotamian Plain provinces of Iraq (Yacoub et al., 2012, in Al-Shwaily and Al-Obaidi, 2019). The rock units found in Iraq during the Miocene period encompass various formations, one of which is the Fatha Formation (Middle Miocene). Busk and Mayo (1918) were the first to describe Fatha formation (Bellen et al., 1959) from the Agha Jari oil field in south-west Iran. The name of the lower Fars Formation was changed to the Fatha Formation in 1992 (Al-Rawi et al., 1992).

It is characterized by containing more than 20 cycles, represented by mudstone, marl, limestone, and blocky gypsum (Al-Khafaji and Al-Hadadi, 2022). The lower contact of the Fatha Formation is with the Jeribe Formation, while the upper contact is with the Injana Formation.

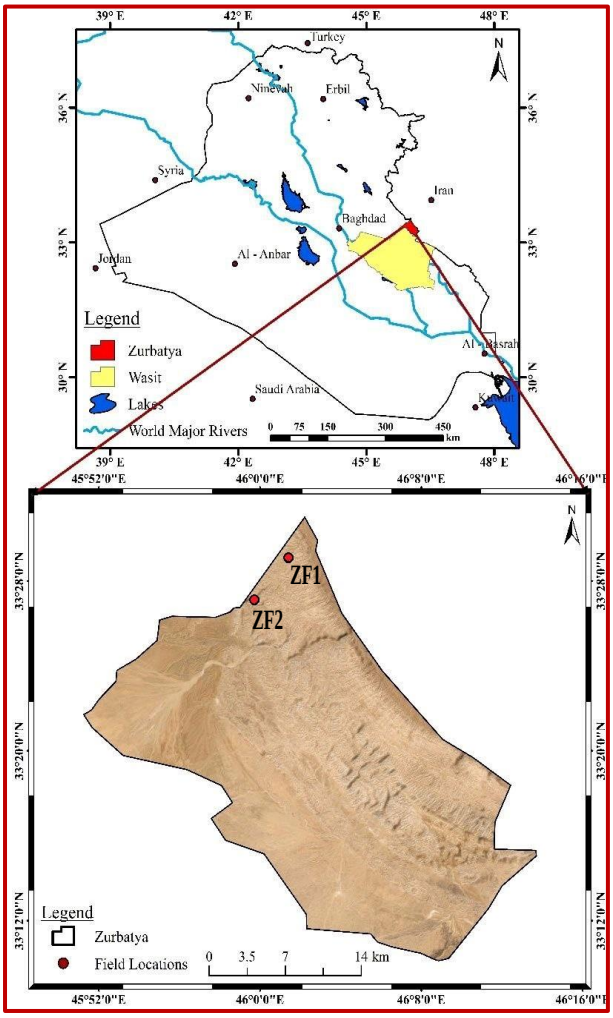

Fig. 1. The location map of the study area

Fig. 2. Fatha Formation at Zurbatiyah area.

Fig. 3. Injana Formation at Zurbatiyah area.

Methodology

Fieldwork

Extensive fieldwork was conducted in the Zurbatiya area, which is located close to Badra city in the Wasit Governorate of eastern Iraq. Limestone samples were gathered from two sections of good exposures, with a wide thickness and lateral extension. Five samples were taken from the Fatha Formation, which is situated in the study area at the coordinates of ZF1 (N 33° 24' 11"/E 45° 57' 06") and ZF2 (N 33° 24' 04"/E 45° 58' 32") (Fig. 1). Two different rock types were used in this study: limestone from the Fatha Formation and mudstone from the Injana Formation. Limestone rocks and claystone vary in extent and thickness, which means they can be used in many areas through open pit mining (Fig. 2) and (Fig. 3).

Laboratory work

The crushing and grinding of the limestone and claystone with agate mortar and passing the sample through a (75 µm) sieve, so that the samples are ready for chemical and mineralogical analysis.

Mineralogical analysis

Five limestone and two claystone samples were analyzed by the XRD technique and scanned with a 2θ range of (5°-65°). The Broker D2 phaser device was used in the Iraqi-German laboratory, University of Baghdad, College of Science, Department of Geology. In addition, two samples were selected to separate and detect insoluble residues according to the standard (ASTM D3042-3, 2004). Furthermore, the clinker produced at Materials and Energy Research Center (MERC), in Tehran, Iran, the clinker samples was analyzed using an XRD technique and scanned with a range of (2θ) from (4°-60°) at Karsarn Binalond Company to determine the minerals of the clinker. To reveal the microstructure and crystalline shape of the clinker phases, the SEM technique was used at the Al-Razi Center for Mineral Research, Tehran, Iran, after coating the samples with gold using a coating cell before examining them with an S360-Cambridge SEM device. The samples were burned and cooled in (Fig. 4).

Fig. 4. A-Samples after burning, B-Clinker product.

Chemical analysis

The major elemental contents of five limestone samples and two claystone samples were analyzed using XRF techniques. The analysis was conducted using the Ed-XRF Instrument Spectro-Xepos of Ametek Company in the Iraqi German Laboratory at the University of Baghdad, College of Science, Department of Geology. Before analysis, 200g of limestone was pulverized and ground using an agate mortar and then sieved to a particle size of 75µm. The primary composition of the clinker was examined using the XRF technique at the Karsarn Binalond Company, Tehran, Iran. The analysis was conducted under conditions of a current of 30 mA and a voltage of 60 kV.

Cement Chemical Parameters

To manufacture cement, a suitable raw mixture must be prepared, which depends on knowing the percentage of oxides that compose the raw materials, which can be determined by XRF analyses. The major oxides are CaO, SiO_2, Al_2O_3, and Fe_2O_3. These oxides play a crucial role in proper burning and achieving the required characteristics of the final product. To balance these oxides, many parameters are required. These parameters are lime saturation factor (LSF), silica ratio (SR), and alumina ratio (AR) (Marzouki et al., 2013).

Lime saturation factor (LSF)

LSF is the molar ratio of CaO to the other three major oxides, SiO_2, Al_2O_3, and Fe_2O_3. LSF for clinker is in the range 92–98 (Rao et al., 2011). It plays a crucial role in feedstock preparation by preventing the use of compositions that surpass the lime's ability to interact with silica, alumina, and ferric oxides elements (Hewlett, 2004). According to (Janamian and Aguiar 2023), LSF can be calculated by the equation:

If (MgO < 2) $$LSF=\frac{CaO+0.75\ MgO}{(2.85*SiO_2+1.18*Al_2O_3+0.65*Fe_2O_3)}\ 100$$

If (MgO > 2) $$LSF=\frac{CaO+1.5}{(2.85*SiO_2+1.18*Al_2O_3+0.65*Fe_2O_3)}\ 100$$

Silica ratio (SR)

SR of clinker within the range between 2 - 3 (Rao et al., 2011). According to Hewlett and Liska (2019), SR can be calculated by the equation:

$$SR=\frac{SiO_2}{(Al_2O_3+Fe_2O_3)}$$

Aluminum Ratio (AR)

AR of clinker acceptable in the range between 1.3 and 2.5 (Taylor, 1997) and between 1 and 4 (Rao et al., 2011). According to Hewlett and Liska (2019), AR can be calculated by the equation:

$$AR=\frac{Al_2O_3}{Fe_2O_3}$$

Results and discussion

Mineralogical analysis

The X-ray diffraction (XRD) analysis of limestone revealed that calcite is the predominant mineral, and quartz in the limestone was relatively low. Limestone samples have a lower amount of dolomite (Figs 5 and 6) due to the low content of magnesium oxide. The XRD analysis revealed that quartz is the predominant mineral found in the insoluble residues (IR) (Fig. 7).

By XRD analysis of the claystone, kaolinite minerals were identified at reflectance at 7.1A°, Illite reflection at 10 A° and 5.0 A°, Palygorskite reflection at 10.5 A°, Chlorite reflection at 4.7 A°, and Mixed layer mineral reflection at 13.39 A° (Fig. 8).

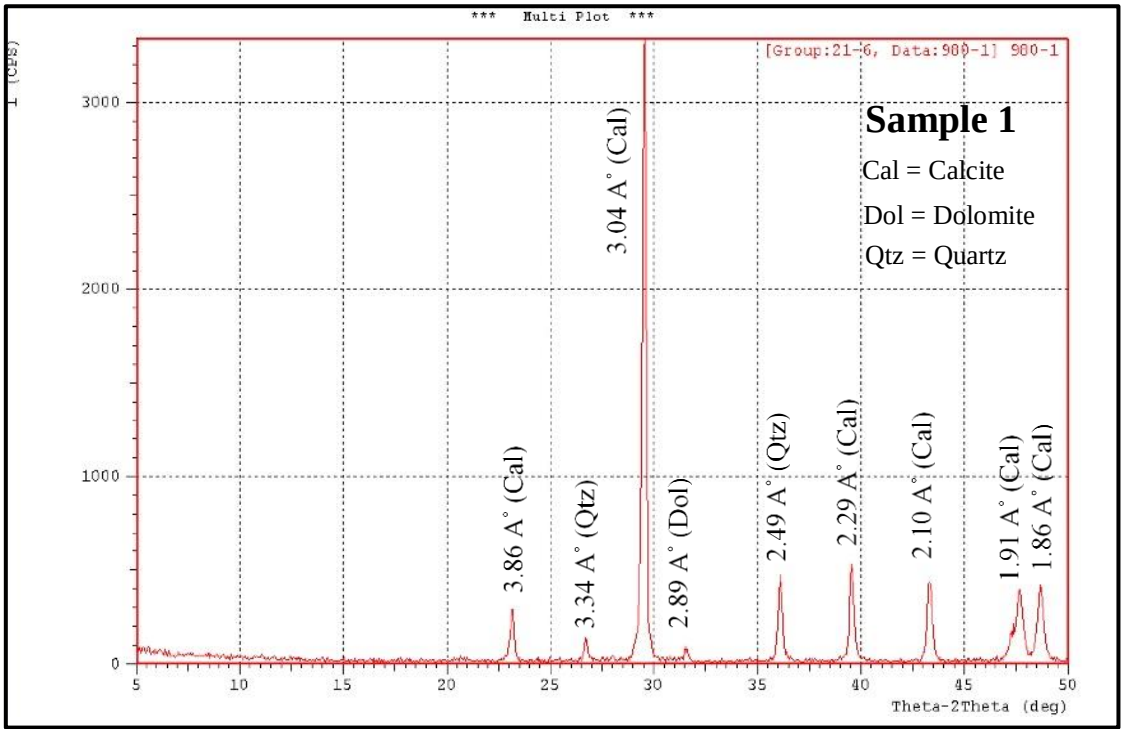

Fig. 5. XRD patterns of Fatha limestone (sample1)

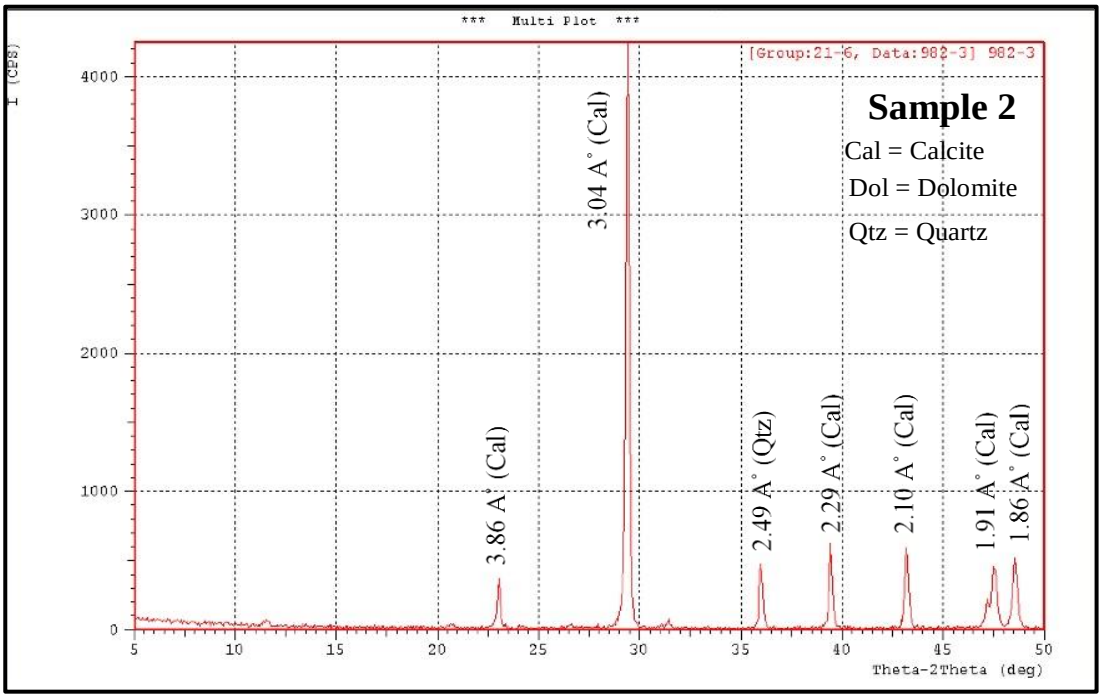

Fig. 6. XRD patterns of Fatha limestone (sample2)

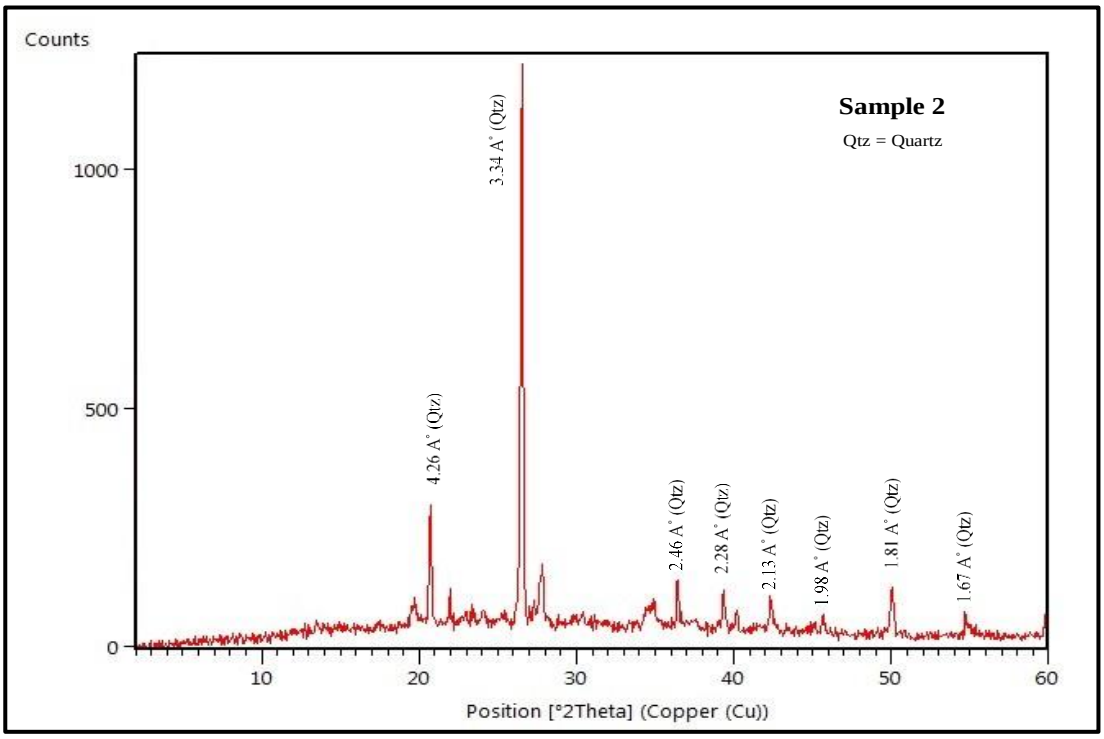

Fig. 7. XRD patterns of insoluble residue of Fatha limestone (sample 2)

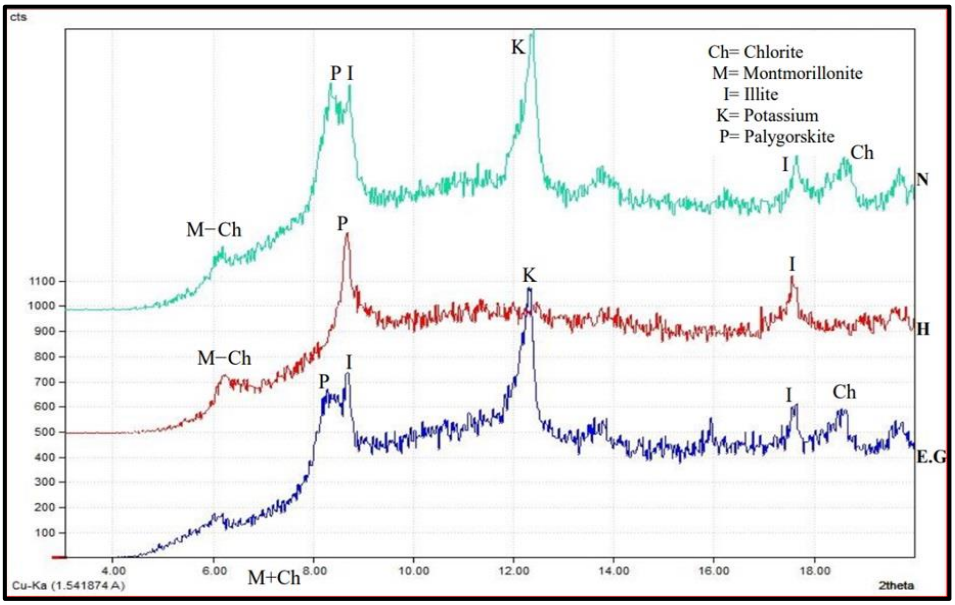

Fig. 8. XRD of claystone sample (Al-Najjari, 2019).

Chemical Analysis:

(Table 1) shows the percentages of major and minor oxides for limestone samples, as follows: CaO ranges from 47.34% to 54.77% with an average of 51.87%. SiO_2 ranges from 2.53% to 9.64% with an average of 4.81%. Al_2O_3 ranges from 0.65% to 2.38% with an average of 1.24%. Fe_2O_3 ranges from 0.41% to 1.14% with an average of 0.69%. MgO ranges from 0.49% to 0.94% with an average of 0.77%. The low value of MgO refers to the dolomitization process that affects the limestone. The maximum percentage of magnesium in OPC is 5%, as established by some standards like IQS No.5 (1984), 6% by ASTM C150-85 (1986), and 4% by BS12 (1989). Although the early strength of cement is improved by the presence of alkaline sulfates, an excess of these sulfates can cause accumulations and cover the kiln's interior walls, which can alter the burning conditions (Duda, 1985). The maximum percentage of sulfate in OPC is 2.5%, as specified by IQS No. 5 (1984), 3% maximum in both BS12 (1989) and ASTM C150-85 (1986). There is also little alkali content (Na_2O and K_2O). The high content of alkalis in cement has a detrimental effect on the cement's quality. The reaction of alkalis with silica tends to increase the volume, which is detrimental to the concrete (Schafer, 1987). The ASTM C150-85 (1986) standard states that the maximum number of alkalis in the cement is 1.6%. Average results of chemical analysis of Injana sediments indicated that the claystone contained 11.81% CaO, 36.40% SiO_2, 10.45% Al_2O_3, 5.33% Fe_2O_3, and 5.37% MgO. The percentage of silica and alumina is low, while the levels of magnesium oxide are high (Table 2), which indicates that it may need to be added to enhance both silica and alumina. In the current investigation of limestone and claystone, most of these oxide percentages are within permissible bounds for raw materials used in the cement industry when compared with (Schorcht et al., 2013).

Table 1: Chemical analysis of limestone samples.

Oxides %		SiO_2	Al_2O_3	Fe_2O_3	K_2O	Na_2O	CaO	MgO	SO_3	L.O.I	Total
Schorcht et al. (2013)		**0.5-50**	**0.1-20**	**0.2-5.9**	**0-3.5**	**0-1.5**	**20-55**	**0.2-6**	**0-0.7**	**2-44**	**-**
Fatha Formation Samples %	1	3.14	1.04	0.80	0.21	0.75	54.00	0.94	0.55	38.55	99.98
	2	5.54	0.65	0.65	0.13	0.69	53.03	0.49	0.65	38.64	99.96
	3	3.20	0.93	0.41	0.03	1.05	54.21	0.79	0.62	38.92	100.16
	4	2.53	1.22	0.47	0.14	0.74	54.77	0.75	0.37	37.97	98.96
	5	9.64	2.38	1.14	0.59	0.77	47.34	0.88	0.62	37.49	100.85
	average	4.81	1.24	0.69	0.22	0.80	51.87	0.77	0.56	38.31	99.98

Table 2: Chemical analysis of claystone samples (after Al-Najjari, 2019).

Oxides %	SiO_2	Al_2O_3	Fe_2O_3	K_2O	Na_2O	CaO	MgO	SO_3	L.O.I	Total
Schorcht et al. (2013) %	**33-78**	**7-30**	**4-15**	**0.4-5**	**0.1-1.5**	**0.2-25**	**0.3-5**	**0-4**	**1-20**	**-**
1	37.40	11.13	5.63	1.80	0.67	11.97	5.55	1.20	24.17	99.52
2	35.40	9.77	5.02	1.59	2.34	11.64	5.19	1.97	27.49	100.41

Injana Formation samples %	average	36.40	10.45	5.33	1.70	1.5	11.81	5.37	1.59	25.83	99.96

Raw mix design

Relying on (Schorcht et al. 2013) as a standard for preparing and designing raw materials, and given that they contain a wide range of raw cement meal, two mixtures were theoretically prepared and designed (Table 3). The first mixture (without additives) conforms to the above-mentioned specification, but another mixture was designed by adding sand and bauxite to obtain a more suitable LSF value while keeping the raw meal oxide values within the limits of the mentioned specification. (Table 4) shows the chemical composition of sand and bauxite used as corrective materials.

Table 3: Chemical composition of the designed raw cement meal

Oxides %			**SiO_2**	**Al_2O_3**	**Fe_2O_3**	**CaO**	**MgO**	**K_2O**	**Na_2O**	**SO_3**
Schorcht et al. (2013) %			**12-16**	**2-5**	**1.5-2.5**	**40-45**	**0.3-5**	**0.1-1.5**	**0.1-0.5**	**0-1.5**
Mix1 %	**Limestone**	73	3.51	0.91	0.5	37.87	0.56	0.16	0.58	0.41
	Claystone	27	9.83	2.82	1.44	3.19	0.86	0.46	0.41	0.43
	Total	100	13.34	3.73	1.94	41.06	1.42	0.62	0.99	0.84
Mix2 %	**Limestone**	75.5	3.63	0.94	0.52	39.16	0.58	0.17	0.60	0.42
	Claystone	21.5	7.83	2.25	1.15	2.54	0.69	0.37	0.42	0.34
	Sand	2	1.74	0.02	0.21	0.02	0	0	0	0.003
	Bauxite	1	0.17	0.61	0.01	0.003	0	0	0.002	0.004
	Total	100	13.37	3.82	1.89	41.72	1.27	0.54	0.92	0.77

Table 4: Chemical composition of correction materials

Oxides% / Material	**SiO_2**	**Al_2O_3**	**Fe_2O_3**	**CaO**	**MgO**	**K_2O**	**Na_2O**	**SO_3**
Sand %	86.75	0.80	0.66	0.76	0.003	0.0012	0.00001	0.15
Bauxite %	16.55	60.78	1.31	0.28	0.004	0.01	0.19	0.38

Clinker preparation

Burning and cooling

The two raw mix ingredients were prepared for a special burning and cooling process, followed by a thirty-minute soaking time at a temperature of 1450 °C. Hot clinker samples were rapidly cooled to 1200 °C and then from 1200°C to room temperature using special program techniques. The process included extracting the clinker from the furnace and expeditiously reducing its temperature. The quality of the finished cement is directly impacted by the clinker cooling process, which also affects the physical characteristics, grinding capacity, and mineral composition (Duda, 1985). It is best to avoid slow cooling as it may lead to relatively large C3A crystals and an increase in Belite content and a reduction in Alite content, and poor rheology in the final product (Newman and Choo, 2003). If the clinker has a high magnesia content, there is a chance that large Periclase grains may crystallize, which affects the quality of cement (Chatterjee, 2018).

Mineralogical analysis of clinker

Subsequent content provides the identification of the main mineral phases in clinker in Mix1 and Mix2 based on Taylor (1997) using X-ray diffraction mineralogical analysis:

Tricalcium silicate (Alite)

Alite (C3S) is the most reactive phase and is the main component of cement, with a range of 50-70%. OPC hydration kinetics is dominated by Alite hydration (Aitcin and Flatt 2016). C3S that is impure is referred to as Alite, and this mineral name encompasses C3S that is present in all commercial clinker (Lamond and Pielert, 2006). The Alite phase exhibits several reflections that are indicative of a rise in its percentage in cement. The Alite phase exhibits its largest reflection at 2.608A˚ and 2.77A˚, in addition to faint reflections at 1.48 A˚ (Fig. 8).

Dicalcium silicate (Belite)

The impure form of Dicalcium silicate (C2S) is the second primary ingredient phase found in Portland clinkers. Usually, Portland clinkers contain 15–38% of it (Brandt, 2009). When lime and SiO_2 combine at the clinkering temperature of 1100 ºC, Belite begins to form (Newman and Choo, 2003). Belite may be found in five different polymorphs, which are α-Belite, α'H-Belite, α'L-Belite, β-Belite (with H representing "high" symmetry and L representing "low" symmetry), and γ-Belite (Telschow, 2012). The existence of the beta polymorphism phase is the most common characteristic of industrial clinkers; however, there are other instances in which the high-temperature forms are present in even smaller quantities. On the other hand, the gamma form exhibits poor hydraulic behavior, while the beta form comes with favorable hydraulic qualities (Chatterjee, 2018). According to Taylor (1997), Alite and Belite are matched in reflections 1.76A˚ and 2.19 A˚; however, Belite may occur at reflection 2.88Ạ. The reflections with a magnitude of 2.448A˚ and 2.403A˚ are generally considered the most useful in determining the Belite phase. There is a possibility that the reflection at 2.448A˚ could sometimes coincide with the feeble reflection of Alite, which is situated at 2.449A˚ (Fig. 9).

Tricalcium aluminate (Celite)

Celite (C3A) makes up 5–10 weight percent of the Portland cement clinker and is its most reactive component. Pure C3A does not show temperature-dependent polymorphs and is composed of 62 weight percent CaO and 38 weight percent Al_2O_3. Polymorphs of orthorhombic and cubic structures are frequently found in industrial clinker products (Telschow, 2012). Aluminate is useful in the production of cement because it forms a liquid during clinkering, which helps Belite and Alite develop in the cement kiln (Ylmén, 2013). Conversely, C3A and its derivatives can cause concrete damage by taking part in expansion reactions that cause tension and cracking (Mistri et al., 2013).

The strong reflection at (2.70A˚) is typically used to differentiate this phase from others; nevertheless, this reflection aligns with the ferrite phase either partially or entirely, making it difficult to characterize this phase. There is a possibility that the presence of alkali or magnesia replacement in the Alite phase may cause interference or slight divergence, leading to the appearance of a higher value. (Stutzman, 1996) (Figs 8 and 9).

Calcium Aluminoferrite (Ferrite)

Ferrite (C4AF) averages about 5-12% of typical clinker (Newman and Choo, 2003). When C3A levels are low, C4AF levels tend to be higher. This is because C4AF and C3A are both liquid at kiln temperatures, and controlling the amount of liquid phase is key to burning clinker and running the kiln (Lamond and Pielert, 2006). It was also observed that as the cooling rate decreased, the degree of crystallization of ferrite from the liquid phase increased (Peterson, 2003). Although this phase has low hydraulic properties. However, it contributes to developing the strength of concrete (Chatterjee, 2018). The phase exhibits a prominent reflection at 2.63 and 2.68A˚, which aligns with the reflection value of 2.70A˚ for Aluminate and 2.608Å for Alite phase (Figs 9 and 10). Additionally, it exhibits a primary intensity reflection between 2.66 and 2.71A˚, but it interferes with Aluminate at a reflection of 2.70 A˚.

(Fig. 11) shows the stages of formation of these phases. Belite (C2S) is formed when lime combines with silica, although the amount of lime that has not yet been reacted remains high until a temperature of approximately 1250°C is attained. Partial melting takes place at around 1300°C, with the liquid phase being supplied by the alumina and iron oxide that are present. As C2S is transformed into C3S, the amount of lime that has not yet reacted decreases. C3S formation is complete at 1450°C.

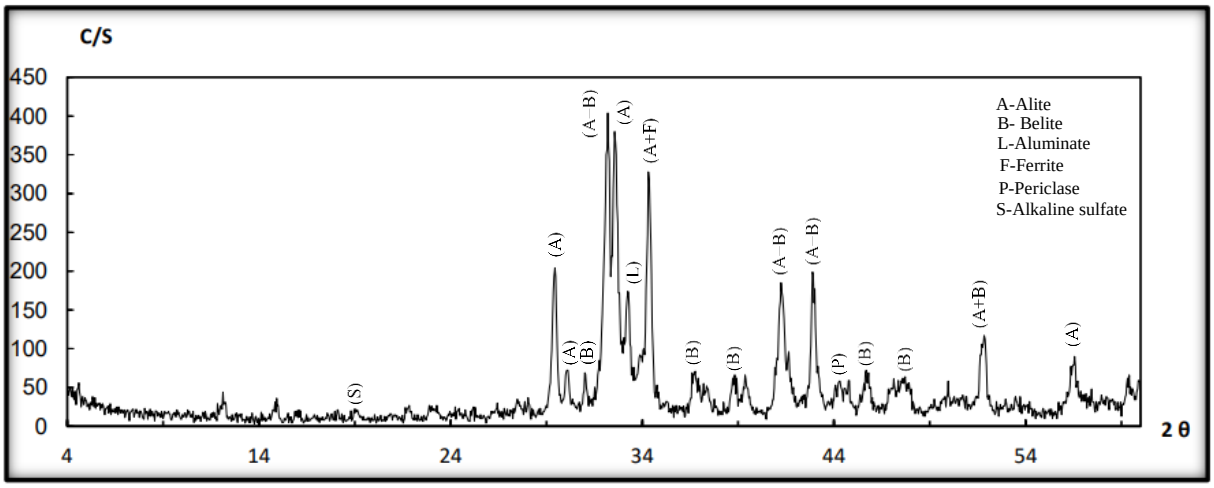

Fig. 9. The XRD patterns for produced clinker Mix1

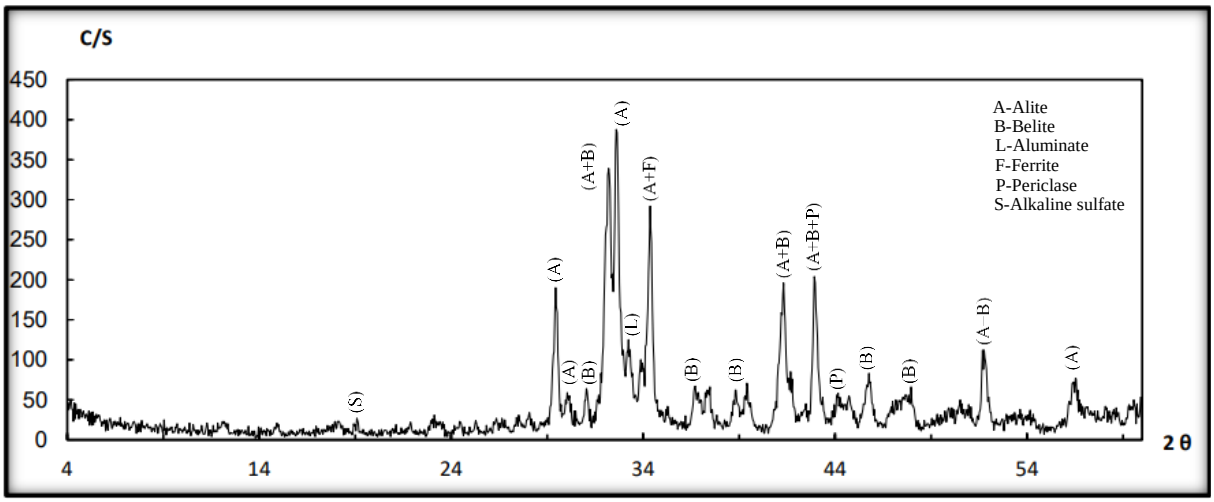

Fig. 10. The XRD patterns for produced clinker Mix2

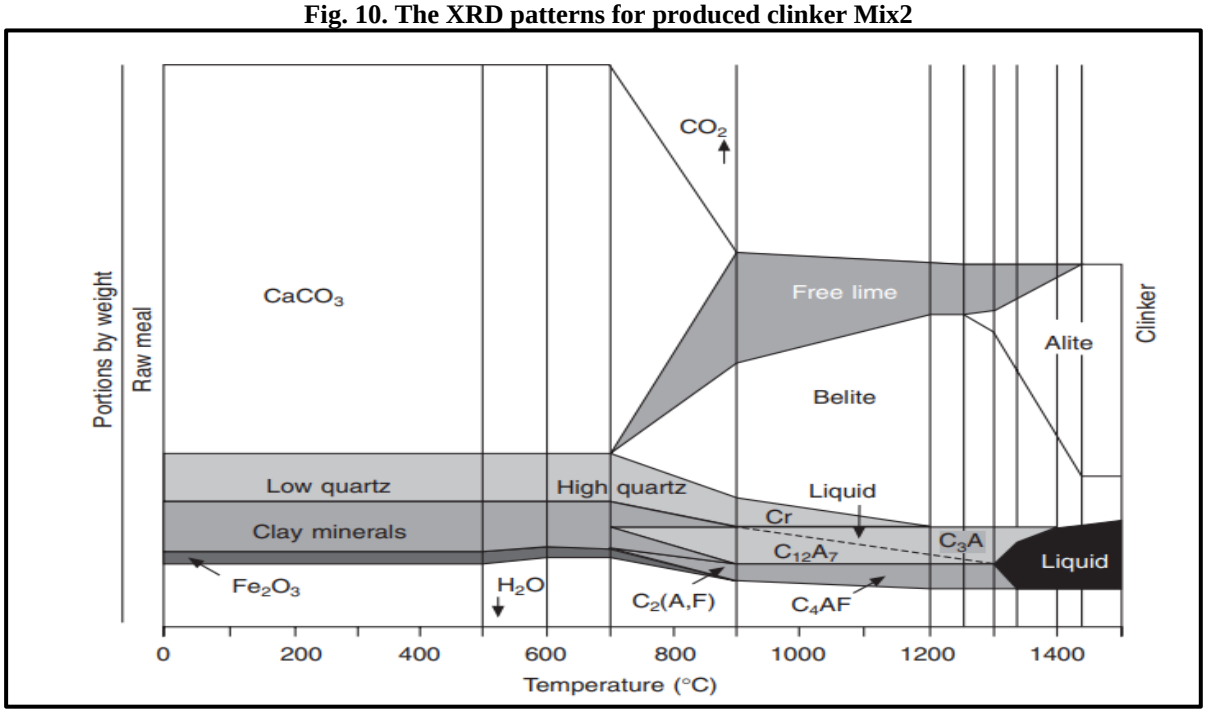

Fig. 11. Clinker formation reactions (Newman and Choo, 2003)

Scanning electron microscopy

Alite

The Alite crystal is the most desirable clinker phase in Portland cement clinker (Ahmadi 2017). Alite may only be formed in conditions when there is an excess of CaO, or when the ratio of CaO to SiO_2 is more than one. Thermodynamically, it must be stable at temperatures above 1250°C (De la Torre, 2007). Alite crystals are idiomorphous, vitreous, and compact. In their cross-section, they usually have six sides, depending on the angle of cut (Pritula et al., 2004). Alite crystals typically range in size from 25 to 65 µm in dimension. (Campbell, 1999) After the clinker, samples were examined using a scanning electron microscope (SEM), and the results showed that the Alite phase crystals appeared in hexagonal form (Plate 1). This crystal may be seen in all of the samples in a characteristic crystalline form.

Belite

The grains of Belite exhibit idiomorphic morphology, displaying a vitreous texture and frequently assuming a rounded form. Furthermore, they possess a unique lamellar structure that extends in multiple directions. At temperatures below 1300°C, the size of Belite particles varies from 1 to 4 µm. However, when exposed to high temperatures of about 1500°C, Belite undergoes recrystallization and its size increases 20 to 40 µm (Campbell, 1999). Belite phase crystals appear as spherical, euhedral crystals with smooth surfaces and transparent laminates under a microscope (Plates 1 and 2).

Tricalcium aluminate

Tricalcium aluminate in clinker with minimal or no alkali content often forms crystals that are uniformly tiny or xeromorphic to rectangular. These crystals can vary in size from 1 to 60 µm (Campbell, 1999). On the other hand, alkaline aluminate tends to crystallize in the form of laminae, which can sometimes resemble laths or long staves (Taylor, 1964) (Plate 2).

Ferrite

Ferrite is distinguished by its high reflectivity, which results in a white look. It comes in either dendritic or lath-like forms (Stutzman and Leigh, 2002) (Plate 1).

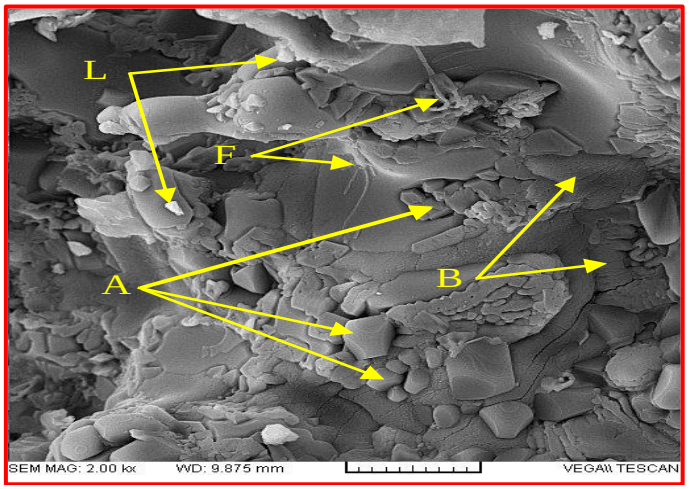

Plate 1. Micrograph by SEM of Mix1, A-Alite, B-Belite, L-Aluminate and F- Ferrite

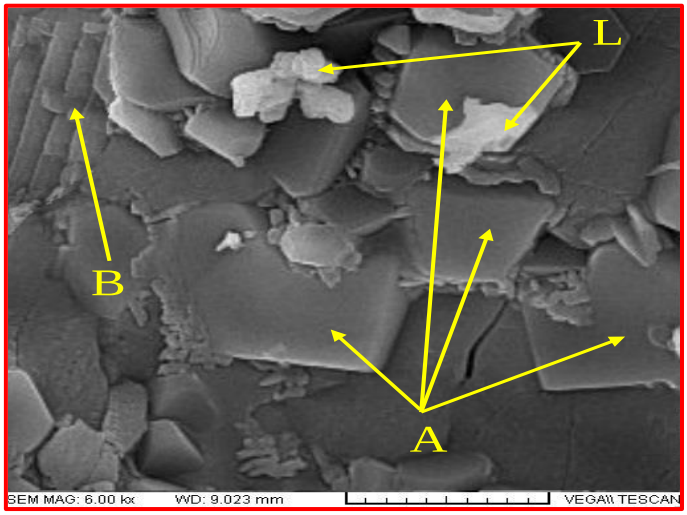

Plate 2. Micrograph by SEM of Mix2, A-Alite, B-Belite, and L-Aluminate

Chemical analysis of clinker

(Table 5) shows the results of the chemical analysis of the oxides constituting the two clinker samples using the XRF technique. The analysis results showed that CaO is the dominant oxide in both mixtures. The percentage of oxides in the first mixture (Mix1) (without additives) was CaO (62.29%), SiO2 (21.38%), Al_2O_3 (5.07%), Fe_2O_3 (2.62%), MgO (3.90%), and SO_3 (2.12%). While it was in the second mixture (Mix2) (with additives) CaO (63.94%), SiO2 (21.46%), Al_2O_3 (5.12%), Fe_2O_3 (2.15%), MgO (3.63%), Finally SO_3 (0.97%), then compared with (Duda, 1985). The chemical parameters (LSF, SR, and AR) were calculated and compared with those (Rao et al. (2011). The additives caused an increase in both silica and alumina oxides, and thus, the percentage of Alite phase increased (Table 5).

Table 5: Chemical analysis of the produce cement clinker

specifications	(Duda, 1985)							(Rao et al., 2011)		
Oxides and parameters %	SiO_2	Al_2O_3	Fe_2O_3	Na_2O +K_2O	CaO	MgO	SO_3	LSF%	SR	AR
specification values	16-26	4-8	2-5	0-1	58-67	1-5	0.1-2.5	92-98	2-3	1-4
clinker product Mix1 %	21.38	5.07	2.62	0.84	62.29	3.90	2.12	92.96	2.78	1.93
clinker product Mix2 %	21.46	5.12	2.15	0.64	63.94	3.63	0.97	95.39	2.95	2.38

Clinker phases

The percentage of each mineral phase likely to be in the clinker was calculated by use of Bogue's formulas. These formulas for the main compounds in the clinker are given below (Table 6).

Table 6: Bogue's equations for calculating the main phases of clinker (Chatterjee, 2018)

Clinker phases	If Al_2O_3 / Fe_2O_3 (alumina ratio) ≥ 0.64	If Al_2O_3 / Fe_2O_3 (alumina ratio) < 0.64
C_3S	$4.071CaO - 7.602SiO_2 - 6.719Al_2O_3 - 1.430Fe_2O_3 - 2.852SO_3$	$4.071CaO - 7.602SiO_2 - 4.479Al_2O_3 - 2.859Fe_2O_3 - 2.852SO_3$
C_3S	$2.867SiO_2 - 0.754C3S$	$2.867SiO_2 - 0.754C_3S$
C_3A	$2.650Al_2O_3 - 1.692Fe_2O_3$	0
C_4AF	$3.043Fe_2O_3$	$2.10Al_2O_3 + 1.702Fe_2O_3$

The results of Bogue calculations for the resulting clinker phases (C3S, C2S, C3A, and C4AF) for Mix1 (47.19, 25.71, 9.00, and 7.97) are shown, respectively. While the Mix2 was (56.92, 20.05, 9.93, and 6.54). Based on (Newman and Choo, 2003), the Mix2 is better than the Mix1 due to the Alite content, as shown in Table 7.

Table 7: Calculations for the main phases and parameters in the clinker of the study.

Clinker Phases	C3S	C2S	C3A	C4AF
Mix1	47.19	25.71	9.00	7.97
Mix2	56.92	20.05	9.93	6.54
Newman and Choo, 2003	45-65	10-30	5-12	6-12

Clinker Properties

Hydraulic Modulus (HM):

It is the lime saturation ratio, but in a more simplified way because all the oxides are taken without their coefficients, the value of HM ranges from 1.9 to 2.4 (Chatterjee, 2018). However, the good quality is 2 (Ghosh, 2002). An increased value of HM signifies a greater demand for energy or a greater thermal load. The hydraulic modulus of clinker can be calculated by applying the equation that is presented below (Sengupta, 2020).

$$CaO/ (SiO_2+ Al_2O_3+ Fe_2O_3)$$

Minimum Burning Temperature (M.P.T)

This parameter represents the lowest temperature in the rotary kiln at which the liquid phase begins to appear (Yezdeen, 1990). Around 20% to 30% of the dry matter is converted into a liquid condition as a result of the melting of the primary compounds in the lower part of the kiln, which occurs at temperatures ranging from 1250° to 1350°C (Naqi and Jang, 2019). According to (Newman and Choo, 2003), the value of MPT, not be less than 1250°C. According to Chatterjee (1979), this coefficient is calculated by the following equation:

$$MBT°C = 1300 + 4.51 * C3S – 3.74 *C3A – 12.64 * C4AF$$

Burnability Index (BI)

BI is referring to the level of ease or difficulty involved in burning the mixture when it enters the rotary kiln and transforming it into clinker. It ranges (2.6-4.5) and can be calculated through the following equation: (Peray and Waddell, 1972)

$$BI = C3S / C3A + C4AF$$

Liquid phase at burning zone (L.Ph):

It refers to the quantity of liquid that is produced at the temperature at which clinker is formed, and it is contingent upon the temperature at which the burning process takes place as well as the chemical makeup of the raw mixture. The liquid phase is necessary for the supplemental materials that are used for melting, which leads to a substantial amount of the liquid phase being present while the burning process occurs, under the conditions, the clinker phases are formed (Al-Ali, 2004).

The percentage of liquid phase that is present in the burning zone ranges from 23% to 28 % (Newman and Choo, 2003). According to Lea-Parker (Gouda, 1979) can be calculated according to the following equations:

$$L.Ph\ \% = 3.0\ Al_2O_3 + 2.25\ Fe_2O_3 + MgO + K_2O + Na_2O + SO_3$$

Viscosity is increased at 1450 °C by Al_2O_3, K_2O, and Na_2O, and decreased by Fe_2O_3 and SO_3 (Mohamed et al., 2018).

HM, MPT, BI, and L.Ph values of the clinker produced are within the permissible limits as shown in Table 8.

Table 8: Properties of produced cement clinker

Clinker Properties	HM	MPT	BI	L.Ph
Mix1	2.14	1378.43	2.78	27.96
Mix2	2.23	1436.91	3.45	25.44
Newman and Choo, 2003	1.7 – 2.3	>1250°C	2.6 – 4.5	23 - 28

Conclusions

1. Fieldwork conducted in the study area showed that the Fatha Formation contains sequences of limestone with good thicknesses and extensions, as well as the Injana Formation, which contains a good amount of claystone. It can be used to produce ordinary Portland cement.

2. Oxides of limestone and claystone are within the specification's limits of raw material for cement manufacturing.
3. The high LSF percentage is evidence of the purity of the limestone. Therefore, the addition of claystone from the Injana Formation in the study area is required to make it conform to international specifications and suitable for manufacturing ordinary Portland cement.
4. Most of the chemical parameters of clinker, including LSF, SR, AR, and Clinker phases (C3S, C2S, C3A, and C4AF), are within the standard specification for the production of Portland cement.
5. Rapid cooling has an effective role in the formation of clinker facies, especially for Alite and Belite, as a result of SEM, which showed the mineral phases of the clinker very clearly.
6. The majority of the properties of the clinker, such as hydraulic modules (HM), minimum burning temperature (MBT), Burnability index (BI), and Liquid phase at the burning zone (L.Ph), are within the parameters of the standard specification for the production of Portland cement.

References

Ahmadi, Z., 2017. Mineralogy and SEM study of Redacting Conditions in the Fars Cement Factory Clinkers (SW Iran). Advances in Applied Science Research, 8(4), pp. 14-20.

Aitcin, P.C., and Flatt, R.J. (Eds.)., 2015. Science and Technology of Concrete Admixtures. Woodhead Publishing. https://shop.elsevier.com/books/science-and-technology-of-concrete-admixtures/aitcin/978-0-08-100693-1.

Al-Ali, N. and Al-Khafaji, S., 2020. Assessment of Limestone of Ibrahim Formation in Zurbatiya Area, Eastern Iraq for Ordinary Portland Cement Industry. Iraqi National Journal of Earth Science, 20(2), pp. 19-32. DOI:10.33899/EARTH.2020.170358.

Al-Ali, S. H. A., 2004. Assessment of Cement Produced at Kufa Cement Plant and the Raw Materials Used in Its Manufacture. Unpublished MSc. Thesis, Science College, Basrah University, Iraq, 124 P. (In Arabic).

Al-Fraji, Y.I. and Al-Khafaji, S.J., 2023. The Suitability of Fatha Clay Deposits for Clay Bricks Industry in Zurbatiya Area, Eastern Iraq. Iraqi Journal of Science, pp. 2325-2341. https://doi.org/10.24996/ijs.2023.64.5.19.

AL-Hadadi, A.S.Y. and AL-Khafaji, S.J., 2020. Mineralogy and Petrography of Fatha Gypsum Rocks in Zurbatiyah Area, Eastern Iraq. Basrah Journal of Science, 38(2), pp. 328-346. DOI: 10.29072/basjs.202029.

AL-Khafaji, S.J. and AL-Hadadi, A.S.Y., 2024. Industrial Assessment of Mineral Deposits of Zurbatiyah Area, Eastern Iraq. Iraqi National Journal of Earth Science (INJES). Under publication.

Al-Khafaji, S.J. and AL-Hadadi, A.S., 2022. The Reality of Mineral Resources in Iraq, Zurbatiya Area as a Case Study. 1st International Conference for Natural Resources in Iraq, 25-28 October, Tikrit University.

Al-Najjari, N.A.K., 2019. Mineralogy, Geochemistry and Provenance of Injana Formation in Selected Area North-East of Iraq (Bazian, Qura dagh and Darbandikhan) and East of Iraq (Zurbatiya and Badra). Unpublished PhD. Thesis, College of Science, University of Basrah, 277 P.

Al-Najjari, N. A. K. and Al-Khafaji, S. J., 2019. Petrographical study of sandstone of Injana Formation in Bazian (Northern Iraq) and Zurbatya (Eastern Iraq). Journal of Basrah Researches (Sciences), 45(2A).

Al-Rawi, Y.T., Sayyab, A.S., Al-Jassim, J.A., Tamar-Agha, M., AlSammarai, A.H., Karim, S.A., Basi, M.A., Hagopian, D., Hassan, K.M., Al-Mubarak, M., Al-Badri, A., Dhiab, S.H., Faris, F.M. and Anwar, F., 1992. New Names for Some of the Middle Miocene Pliocene Formations of Iraq (Fatha, Injana, Mukdadiya and Bai Hassan formations). Iraqi Geology Journal, Vol. 25, No. 1, pp. 1-7.

Al-Shwaily, A.K. and Al-Obaidi, M.R., 2019. Paleostress Analysis of Neogene Rocks in Zurbatiyah Area, E Iraq. Iraqi Bulletin of Geology and Mining, 15(1), pp. 43-57. https://www.iasj.net/iasj/article/159992.

ASTM D3042-3, 2004. Standard Test Method for Insoluble Residue in Carbonate Aggregates.

ASTM C150-85, 1986. Standard Specification for Portland Cement. pp.152-158, In: Annual Book of ASTM Standards, Vol. 04.02.

Bellen, R.C. Van, Dunnington, H.V., Wetzel, R. and Morton, D., 1959. Lexique Stratigraphique Internal Asie. Iraq. Intern. Geol. Conger. Comm. Stratigr, 3, Fasc. lOa, 333 P.

Brandt, A.M., 2009. Cement-Based Composites. 2nd Ed., Taylor and Francis, London, UK. 536 P. https://doi.org/10.1201/9781482265866.

BS, 12, 1989. British standard specification for Portland cements. Part 1, 5 P.

Busk, H. G., and Mayo, H. T., 1918. Some Note of the Geology of Persian Oilfields. Journal of the Institute of Petroleum Technology, Vol . 5, pp. 5-26.

Campbell, D.H., 1999. Microscopical Examination and Interpretation of Portland Cement and Clinker. 2nd Ed., Portland Cement Association, 202 P. https://cir.nii.ac.jp/crid/1130000795767341312 .

Chatterjee, A.K., 1979. Cement Raw Materials and Raw Mixes. A Review of Diagnostic Interrelations. The Physico-Chemical Characteristics of Raw Materials and the Reactivity of Raw Mixes. Jour. Pit and Quarry. Part, Sept., part 2, Nov., pp. 103-111.

Chatterjee, A.K., 2018. Cement Production Technology: Principles And Practice. Taylor and Francis, London, New York. 419 P. https://doi.org/10.1201/9780203703335.

De la Torre, Á. G., Morsli, K., Zahir, M., and Aranda, M. A., 2007. In Situ Synchrotron Powder Diffraction Study of Active Belite Clinkers. Journal of Applied Crystallography, 40(6), pp. 999-1007. https://doi.org/10.1107/S0021889807042379.

Duda, W.H., 1985. Cement-Data-Book. International Process Engineering in the Cement Industry, 3rd Ed., Bauverlag, GmbH. Wiesbaden and Berlin, Macdonald and Evans, London, 539 P.

Gambhir, M.L., 2013. Concrete Technology: Theory and Practice. Tata McGraw-Hill Education.

Ghosh, S.N., 2002. Advances in Cement Technology, Chemistry, Manufacture and Testing. 2nd Ed., Tech. Books International, New Delhi, India. 804 P.

Gouda, G.R., 1979, Raw Mix: the Key for a Successful and Profitable Cement Plant Operation, World Cement Technology, Vol. 10, No.10, pp. 337-346.

Hewlett, P.C., 2004. Lea's Chemistry of Cement and Concrete. 4th Ed., Elsevier Science and Technology Books, 1066 P. https://shop.elsevier.com/books/leas-chemistry-of-cement-and-concrete/hewlett/978-0-7506-6256-7.

Hewlett, P. and Liska, M., 2019. Lea's Chemistry of Cement and Concrete. 5th Ed., Butterworth-Heinemann, 880 P. https://shop.elsevier.com/books/leas-chemistry-of-cement-and-concrete/hewlett/978-0-08-100773-0.

Imam, M. and Amin, M., 2007. Materials Properties and Tests, 271 P. (In Arabic).

IQS, No.5, 1984. Iraqi Standard Specification, Portland Cement. (In Arabic).

Janamian, K. and Aguiar, J., 2023. Concrete Materials and Technology: A Practical Guide. CRC Press. https://doi.org/10.1201/9781003384243.

John, J.P., 2020. Parametric Studies of Cement Production Processes. Journal of Energy, 2020, pp. 1-17. https://doi.org/10.1155/2020/4289043.

Khalaf, Y.I. and Al-Khafaji, S.J., 2021. Manufacturing of Environmentally Friendly and Low-Cost Bricks Using Clay Deposits in Zurbatiya Area, Eastern Iraq. Design Engineering, 10984-11001.

Lamond, J.F. and Pielert, J.H., 2006. Significance of Tests and Properties of Concrete and Concrete-Making Materials, Vol. 169, ASTM International.

Marzouki, A., Lecomte, A., Beddey, A., Diliberto, C. and Ouezdou, M.B., 2013. The Effects of Grinding on the Properties of Portland-Limestone Cement. Construction and Building Materials, 48, pp. 1145-1155. https://doi.org/10.1016/j.conbuildmat.2013.07.053.

Mistri, H., Nandoliya, T., Patel, D., Patel, D., Patel, J., and Raval, V., 2013. Cement Industry. MSc. Thesis, a Research Report for Management Research Project-I, V. M. Patel Institute of Management, Ganpat University, 146 P.

Mohamed, Y.A., Kasif, A.E.M.O., Alla, E.A.A. and Elmahadi, M.M., 2018. Calculation of the Formation Process of Clinker Inside the Rotary Cement Kiln. Proceedings of the Voronezh State, University of Engineering Technologies, 80(1), pp. 233-239.

Naqi, A. and Jang, J.G., 2019. Recent Progress in Green Cement Technology Utilizing Low-Carbon Emission Fuels and Raw Materials: A Review. Sustainability, 11(2), pp. 537. https://doi.org/10.3390/su11020537.

Newman, J. and Choo, B.S., 2003. Advanced Concrete Technology; Constituent Materials. 1st edition, Butterworth Heinemann, Elsevier, UK, 288 P. https://shop.elsevier.com/books/advanced-concrete-technology-1/newman/978-0-08-048998-8.

Peray, K.E. and Waddell, J.J., 1972. The Rotary Cement Kiln, Chemical Publishing Co., Inc., New York, 194 P.

Peterson, V.K., 2003. Diffraction Investigation of Cement Clinker and Tricalcium Silicate Using Rietveld Analysis. Unpub. PhD. Thesis, Materials and Forensic Sciences, University of Technology, Sydney, 130 P.

Pritula, O., Smrčok, Ľ., Többens, D. M. and Langer, V., 2004. X-Ray and Neutron Rietveld Quantitative Phase Analysis of Industrial Portland Cement Clinkers. Powder Diffraction, 19(3), pp. 232-239. DOI: https://doi.org/10.1154/1.1782652

Rao, D.S., Vijayakumar, T.V., Prabhakar, S. and Raju, G.B., 2011. Geochemical Assessment of a Siliceous Limestone Sample for Cement Making. Chinese Journal of Geochemistry, 30(1), pp. 33-39. https://doi.org/10.1007/s11631-011-0484-8.

Schafer, H.U., 1987. Assessment of Raw Materials for the Cement Industry. Reprinted from the Journal World Cement. Cement and Concrete Association, London, 7, pp. 273-283. https://pascal-francis.inist.fr/vibad/index.php?action=getRecordDetail&idt=7570850.

Schorcht, F., Kourti, I., Scalet, B.M., Roudier, S. and Sancho, L.D., 2013. Best Available Techniques (BAT) Reference Document for the Production of Cement, Lime and Magnesium oxide. European Commission Joint Research Centre Institute for Prospective Technological Studies (Report EUR 26129 EN). Luxembourg: Publications Office of the European Union, 506 P. DOI: 10.2788/12850

Sengupta, P., 2020. Refractories for the Cement Industry, pp. 185-192, Cham, Switzerland: Springer. https://link.springer.com/book/10.1007/978-3-030-21340-4.

Shabana, N., 2013. Cement Rotary Kiln. Qatar National Cement Company, pp. 1-2.

Stutzman, P. and Leigh, S., 2002. Phase Composition Analysis of the NIST Reference Clinkers by Optical Microscopy and X-Ray Powder Diffraction. NIST technical note, 1441, 44.

Stutzman, P.E., 1996. Guide for X-Ray Powder Diffraction Analysis of Portland Cement and Clinker. NISTER 5755, 38 P.

Taylor, H.F.W., 1964. The Chemistry of Cement, Vol. 1, Academic Press, London and New York, 460 P.

Taylor, H.F.W., 1997. Cement Chemistry. 2nd Ed., Thomas Telford, London, UK, 459 P.

Telschow, S., 2012. Clinker Burning Kinetics and Mechanism. Unpup. PhD. Thesis, Kgs. Lyngby: Technical University of Denmark (DTU), 180 P.

Yacoub, S.Y., Othman, A.A., and Kadim, T.H., 2012. Geomorphology of the Low Folded Zone. Iraqi Bull. Geol. Min., Special Issue, No.5, pp. 7-37, In: Al-Obaidi, M.R. and Al-Shwaily, A.K., 2019. Paleostress Analysis of Neogene Rocks in Zurbatiyah Area, E Iraq. Iraqi Bulletin of Geology and Mining, 15(1), pp. 43-57. https://ibgm-iq.org/ibgm/index.php/ibgm/article/view/221.

Yezdeen, M.E., 1990. Assessment of Some Tertiary Rocks in Wadi Khan-Sinjar Area for the Production of Ordinary Portland Cement. Unpub. MSc. Thesis, College of Science, Mosul University, 197 P. (In Arabic).

Ylmén, E.R., 2013. Early Hydration of Portland Cement. An Infrared Spectroscopy Perspective Complemented by Calorimetry and Scanning Electron Microscopy, Chalmers. University of Technology, 58 P. https://www.proquest.com/openview/d631e90dc3735c5ad4e968f8a609a75a/1?pq-origsite=gscholar&cbl=18750&diss=y.